Molecular Biology of the Cell
Vol. 18, 4327–4342, November 2007

# Neurabin-I Is Phosphorylated by Cdk5: Implications for Neuronal Morphogenesis and Cortical Migration[D]

**Frédéric Causeret,* Tom Jacobs,* Mami Terao,† Owen Heath,* Mikio Hoshino,† and Margareta Nikolić***

*Department of Cellular and Molecular Neuroscience, Imperial College School of Medicine, Charing Cross Campus, London W6 8RP, United Kingdom; and †Department of Pathology and Tumor Biology, Graduate School of Medicine, Kyoto University, Sakyo-ku, Kyoto 606-8501, Japan

Submitted April 25, 2007; Revised July 23, 2007; Accepted August 8, 2007
Monitoring Editor: Paul Forscher

**The correct morphology and migration of neurons, which is essential for the normal development of the nervous system, is enabled by the regulation of their cytoskeletal elements. We reveal that Neurabin-I, a neuronal-specific F-actin–binding protein, has an essential function in the developing forebrain. We show that gain and loss of Neurabin-I expression affect neuronal morphology, neurite outgrowth, and radial migration of differentiating cortical and hippocampal neurons, suggesting that tight regulation of Neurabin-I function is required for normal forebrain development. Importantly, loss of Neurabin-I prevents pyramidal neurons from migrating into the cerebral cortex, indicating its essential role during early stages of corticogenesis. We demonstrate that in neurons Rac1 activation is affected by the expression levels of Neurabin-I. Furthermore, the Cdk5 kinase, a key regulator of neuronal migration and morphology, directly phosphorylates Neurabin-I and controls its association with F-actin. Mutation of the Cdk5 phosphorylation site reduces the phenotypic consequences of Neurabin-I overexpression both in vitro and in vivo, suggesting that Neurabin-I function depends, at least in part, on its phosphorylation status. Together our findings provide new insight into the signaling pathways responsible for controlled changes of the F-actin cytoskeleton that are required for normal development of the forebrain.**

## INTRODUCTION

The dynamic organization of actin filaments is key for the correct morphology, migration, and function of neurons and consequently the normal development of the nervous system. It is therefore important to identify and understand the role of proteins that directly or indirectly control actin dynamics in differentiating neurons. Our study focuses on Neurabin-I (Nb1), a 180-kDa neuronal specific scaffolding protein. Nb1 was initially purified and identified based on its ability to bind and cross-link F-actin (Nakanishi *et al.*, 1997). Its F-actin–binding domain is located in the N-terminal region (amino acids 1-144), followed by a PDZ domain, a coiled-coiled region, and a sterile alpha motif (SAM) domain in the C-terminus. Nb1 interacts with a number of cytoplasmic and transmembrane proteins, which it is thought to target to the F-actin cytoskeleton. Nb1 also has the ability to homodimerize or heterodimerize with its close relative Neurabin-II/Spinophilin (Oliver *et al.*, 2002). Therefore the functional consequence of Nb1 activity is most likely the formation of multiprotein complexes that act to regulate the F-actin cytoskeleton.

Previous studies have shown that Nb1 affects stress fiber formation when expressed in nonneuronal cell lines (Oliver *et al.*, 2002), whereas in neurons Nb1 can promote the formation of filopodia-like extensions (Oliver *et al.*, 2002; Terry-Lorenzo *et al.*, 2005). Nb1 is thought to induce dendritic spines by binding to and thus recruiting the Rho GTPase exchange factor (GEF) Lfc, which in turn facilitates localized Rho dependent F-actin reorganization (Ryan *et al.*, 2005). Nb1 also binds Kalirin-7, a Rac1 GEF known to affect dendritic spine morphology, although the functional significance of this interaction has not yet been established (Penzes *et al.*, 2001). Furthermore, Nb1 controls the maturation of dendritic spines, in this manner modulating synaptic transmission (Zito *et al.*, 2004; Terry-Lorenzo *et al.*, 2005). Consistent with a role of Nb1 in synaptic plasticity, Nb1 knockout mice exhibit deficits in long-term potentiation at corticostriatal synapses (Allen *et al.*, 2006). Interestingly, Nb1 regulates the subcellular localization and activity of the protein phosphatase 1 (PP1), which also has important implications on cellular morphology as well as postsynaptic function (McAvoy *et al.*, 1999; Oliver *et al.*, 2002; Terry-Lorenzo *et al.*, 2005).

The first indication that Nb1 may be important for earlier stages of neuronal differentiation came from subcellular localization studies. Nb1 was found enriched in axonal growth cones of immature hippocampal neurons, where loss of function caused by exposure to antisense phosphorothioate oligonucleotides resulted in inhibition of neurite outgrowth (Nakanishi *et al.*, 1997). Nb1 was subsequently shown to be required for Rac3-dependent neuritogenesis (Orioli *et al.*, 2006). More recently, NAB-1, the *Caenorhabditis elegans* homolog of Nb1, was shown to be essential for the correct establishment of neuronal polarity (Hung *et al.*, 2007). In its absence, synaptic vesicles were not restricted to the axon, but were also found in dendrites. Although these findings

This article was published online ahead of print in *MBC in Press* (http://www.molbiolcell.org/cgi/doi/10.1091/mbc.E07–04–0372) on August 15, 2007.

[D] The online version of this article contains supplemental material at *MBC Online* (http://www.molbiolcell.org).

Address correspondence to: Margareta Nikolić (m.nikolic@imperial.ac.uk).

indicate a role for Nb1 in neurons before synaptic regulation, currently much remains unknown concerning its function in the developing nervous system. We now reveal that normal neuronal morphology, migration, and neurite outgrowth depend on the balanced activity of Nb1 which is, at least in part, controlled by the Cdk5 kinase.

Cdk5 is a proline-directed serine/threonine kinase identified more than a decade ago (Lew *et al.*, 1992; Meyerson *et al.*, 1992). It is activated by association with a regulatory partner p35 or p39, which is highly enriched in neurons (Dhavan and Tsai, 2001). Cdk5 is essential for a number of major developmental processes, particularly radial migration of neurons in the cerebral cortex. Thus mice deficient for *cdk5* or *p35* expression are characterized by an inverted cerebral cortex where neurons that should locate closer to the pial surface reside in more ventral positions (Ohshima *et al.*, 1996; Chae *et al.*, 1997). The role of Cdk5 in early migratory events including splitting of the preplate is also becoming apparent (Rakic *et al.*, 2006). In addition to controlling neuronal migration, numerous studies have implicated Cdk5 in neurite outgrowth, guidance, and synaptic function (Dhavan and Tsai, 2001), as well as in neurodegenerative processes, particularly Alzheimer's disease (Cheung *et al.*, 2006).

In recent years, the identification of many Cdk5 substrates has brought significant insight into the mechanisms through which it exerts its function. Notably, phosphorylation of the focal adhesion kinase (FAK) and Doublecortin by Cdk5 was shown to be essential for the organization of microtubules in migrating neurons (Xie *et al.*, 2003; Tanaka *et al.*, 2004). Cdk5 has also been suggested to regulate actin dynamics (Humbert *et al.*, 2000). This hypothesis has recently been strengthened by the demonstration that Cdk5 controls dendritic spine morphology by phosphorylating the actin-binding protein WAVE1 and the Rho GTPase activator ephexin1 (Kim *et al.*, 2006; Fu *et al.*, 2007). Furthermore, p27kip1 phosphorylation by Cdk5 indirectly affects actin organization in migrating cortical neurons (Kawauchi *et al.*, 2006). Currently no other molecular mechanisms are known that link Cdk5 activity with regulated changes of the F-actin cytoskeleton during neuronal migration.

Our study reveals an important role of Nb1 in the developing forebrain. We demonstrate both in vitro and in vivo that Nb1 is targeted by Cdk5, which modifies its ability to associate with F-actin. The demonstrated link between Cdk5 and the F-actin cytoskeleton acts to deepen our understanding of the molecular mechanisms required for normal neuronal development.

## MATERIALS AND METHODS

### *In Situ Hybridization*

In situ hybridization was carried out on cryosections as previously described (Myat *et al.*, 1996). Briefly, sections were hybridized over night at 72°C in 50% formamide, 5× SSC, 5× Denhardt's solution, and 250 μg/ml yeast tRNA. The digoxigenin-labeled riboprobe used to detect Nb1 mRNA was obtained by in vitro transcription using a digRNA labeling mix and T7 polymerase (Roche, Indianapolis, IN). The template for transcription was constructed by inserting a fragment of Nb1 cDNA (bases 2339–3158) into pBluescript SK+ (Stratagene, La Jolla, CA) previously digested by SacI and XhoI. The probe was revealed using an anti-digoxigenin antibody conjugated to alkaline phosphatase and the substrate NBT/BCIP (Roche).

### *DNA Constructs*

Neurabin-I cDNA was obtained from Yoshimi Takai (Osaka University; Nakanishi *et al.*, 1997) The S95A mutation was introduced using the Stratagene Quickchange site-directed mutagenesis kit with the following primer (mutated base is underlined): GAAAGGTAGGCCCTCAGCCCCTCAGAAGAGGATG. The wild-type and mutated sequences were subcloned into pCAG-IRES-EGFP vector (Kawauchi *et al.*, 2003).

Nb1$^{1\text{-}287}$ wild-type and A95 were obtained by PCR amplification with the following primers: 5′-GGGAGATCTTTGAAAGCTGAATCTTCAGGT-3′ and 5′-GGGGGATTCTCAGGTACCTTTCTGAGCCAC-3′. The resulting fragments were subcloned into the BglII and BamHI sites of pEGFP-C1 (Clontech, San Jose, CA).

Wild-type and A95 Nb1 actin-binding domain (amino acids 1-144) coding sequences were cloned in pGEX4T2 (Amersham Pharmacia Bioscience, Piscataway, NJ) using BamHI and EcoRI sites, to allow bacterial production of glutathione-*S*-transferase (GST)-tagged proteins (referred to as GST-Nb1$^{1\text{-}144}$ and GST-Nb1A95$^{1\text{-}144}$).

Short hairpin RNA (shRNA) expression plasmids were based on pmU6pro (Yu *et al.*, 2002; Kawauchi *et al.*, 2006). Two construct were designed against noncoding sequences unique to *nb1* mRNA (sh1: 5′-GUGUUGAAUGCACUCUUGAU-3′ and sh2: 5′-GUAGGCGGUUAAAGAACUGU-3′) and one control that contained a sequence that did not match any known transcripts (5′-GAUGGAUCGAUAUAGUGAGU-3′).

### *Cell Culture*

Cortical and hippocampal neurons were obtained from embryonic day (E) 17 to E19 Sprague Dawley rat embryos, dissociated in papain (Sigma, St. Louis, MO), and transfected using Amaxa's (Cologne, Germany) rat neuron nucleofector kit following the manufacturer's instructions. They were plated at a density of 1–5 × $10^4$/cm$^2$ on dishes previously coated with 16 μg/ml poly-D-lysine (Sigma) and 5 μg/ml laminin (Sigma), and cultured in Neurobasal medium (Invitrogen, Carlsbad, CA) supplemented with B27 (Invitrogen), 2 mM L-glutamine (Invitrogen), 1 mM sodium pyruvate (Invitrogen), 0.06 mg/ml cysteine (Invitrogen), and 100 IU/ml penicillin and 100 μg/ml streptomycin (Invitrogen) at 37°C and 5% $CO_2$.

### *Antibodies*

For Western blotting, the following commercial antibodies were used: anti-Cdk5, clone C-8 (Santa Cruz Biotechnology, Santa Cruz, CA), anti-Nb1 (Transduction Laboratories, Lexington, KY), anti-actin (Chemicon, Temecula, CA), anti-Rac1 (Upstate Biotechnology, Lake Placid, NY), anti-α-tubulin, clone B-5-1-2 (Sigma).

To generate Nb1 S95 phospho-specific antibody (anti-pS95Nb1), polyclonal rabbit antisera were collected after immunization with the phosphorylated peptide KGRS<u>S</u>PQKRM (the phosphorylated serine residue is underline) and subjected to affinity purification (procedure implemented by CovalAb, Cambridge, United Kingdom). The antibody obtained gave good immunoreactivity on Western blots after total Nb1 immunoprecipitation. Straight Western blots revealed cross-reactivity with uncharacterized proteins, thus preventing reliable use for immunostaining. Secondary antibodies conjugated to HRP were purchased from Vector Laboratories (Burlingame, CA).

For immunostaining, the following commercial antibodies were used: anti-green fluorescent protein (GFP; Molecular Probes, Eugene, OR), anti-βIII-tubulin (TUJ1, BAbCO, Richmond, CA), anti-MAP2, clone AP20 (Sigma), and anti-dephospho Tau (Tau-1, Chemicon). Secondary antibodies conjugated to Alexa 488, 568, or 633 were purchased from Molecular Probes.

Alexa 568–conjugated phalloidin (Molecular Probes) was used to allow F-actin visualization and DAPI (Vector Laboratories) was used at 1 μg/ml to stain cell nuclei.

### *Imaging and Quantification*

Images were acquired either with a Nikon TE2000-U microscope (Melville, NY) and a Hamamatsu ORCA-ER camera (Bridgewater, NJ), or a Leica TCS SP/UV confocal microscope (Deerfield, IL). Measurements were performed using Openlab and Volocity software (Improvision, Lexington, MA). For neurite outgrowth and branching measurement, processes shorter than 10 μm were not taken into account.

Quantifications were performed with a minimum of 200 neurons from three different experiments for each condition. In most cases, measurements were normalized to allow comparison between experiments, and results were expressed in percentages of control. Data are presented using cumulative distributions diagrams and/or histograms (mean ± SEM). Both Student's *t* test and nonparametric Kolmogorov-Smirnov test were used, and differences were considered significant when $p < 0.05$ for both tests.

### *Kinase Assays*

Recombinant GST-Nb1$^{1\text{-}144}$ and GST-Nb1A95$^{1\text{-}144}$ proteins were produced and subjected to radioactive kinase assay as described previously (Rashid *et al.*, 2001).

### *Rac1 Activity Assay*

Cells were lysed in 20 mM Tris, pH 7.2, 150 mM NaCl, 2 mM $MgCl_2$, 0.5% NP-40, and 1 mM dithiothreitol (DTT) with Complete protease inhibitors (Roche), 1 mM phenylmethylsulfonyl fluoride (PMSF), 10 mM NaF, and 1 mM $Na_3VO_4$. Lysates were incubated in the presence of recombinant GST-Pak1$^{67\text{-}150}$ bound to glutathione-Sepharose beads (Amersham Pharmacia Bioscience). GST-

Pak1$^{67-150}$ only interacts with the GTP-bound (active) form of Rac1. The beads were then collected by centrifugation, washed, and subjected to Western blotting.

### *Actin Assays*

To phosphorylate recombinant GST-Nb1$^{1-144}$, p35/Cdk5 complexes were isolated from Cos7 cells transfected with p35 and Cdk5 expression constructs. Cos7 cells were lysed in 25 mM Tris, pH 7.5, 150 mM NaCl, 5 mM EDTA, 1% Triton X-100, and 10% glycerol with Complete protease inhibitors (Roche), 1 mM PMSF, 10 mM NaF, and 1 mM $Na_3VO_4$. Immunoprecipitation was carried out using 3 $\mu$l of anti-p35 and protein A-Sepharose beads (Amersham Pharmacia Bioscience). The beads were rinsed in kinase buffer and tested for the presence of p35 and Cdk5 through Western blot.

GST-Nb1$^{1-144}$ was incubated 30 min at 37°C in the presence of the beads and 5 mM ATP in kinase buffer. Efficiency of the reaction was assessed by Western blotting using the anti-pS95Nb1 antibody.

F-actin was prepared using the actin-binding spin-down assay kit (Cytoskeleton, Denver, CO), incubated with GST-Nb1$^{1-144}$ and spun down following the manufacturer's instructions. The amount of GST-Nb1$^{1-144}$ cosedimenting with the F-actin filaments was then assessed through Western blotting.

Actin polymerization was performed using pyrene-conjugated actin after the manufacturer's instructions (Cytoskeleton).

### *In Utero Electroporation*

In utero electroporation was carried out as previously described (Kawauchi *et al.*, 2003). Briefly, pregnant ICR mice were purchased from SLC Japan (Sizuoka, Japan) and handled in accordance with guidelines established by Kyoto University. DNA was electroporated into E14.5 mouse embryo cortices, and the embryos were allowed to develop in utero until birth. At postnatal day (P) 0 the electroporated brains were dissected and fixed in 4% paraformaldehyde, cryopreserved in 10% sucrose in 0.12 M phosphate buffer, pH 7.4, embedded in 7.5% gelatin, 10% sucrose in 0.12 M phosphate buffer, pH 7.4, and frozen in isopentane cooled at −55°C. Sections at 20 $\mu$m were obtained and subjected to immunostaining. Cortical layers were distinguished using DAPI and MAP2 staining, and GFP-positive neurons were counted in each layer.

## RESULTS

### *Neurabin-I Is Expressed during Critical Steps of Brain Development*

To determine the possible involvement of Nb1 during embryonic neuronal development, we examined its expression levels and distribution throughout the brain. We performed in situ hybridizations on 14–18-d-old (E14–E18) embryonic brain cryosections, using a digoxigenin-labeled antisense RNA probe. Specific enrichment of *nb1* transcripts could be detected in several regions of the brain. In the cerebral cortex and hippocampus, low levels were observed in the proliferating ventricular zones. At E16 and E18, up-regulation of *nb1* mRNA marked the expansion of postmitotic zones in the cortical and hippocampal plates (Figure 1, A and B). Other regions such as the thalamus, arcuate nucleus in the hypothalamus (Figure 1C, expression detectable as early as E11) and the inferior olive in the hindbrain (Figure 1D) also showed enhanced *nb1* expression. However, it is important to note that *nb1* expression is most likely not restricted to these specific regions as surrounding areas exhibited diffuse staining that was absent in sections hybridized with the control probe (showing virtually no staining; compare Figure 1, A–D, with E). We confirmed these findings in the neocortex by examining the Nb1 protein expression pattern in extracts from E12 to adult mouse cortices (Figure 1F). Low levels of Nb1 were detectable at E14 followed by a dramatic upregulation at E16. Expression peaked from E18 to P1, followed by a gradual decrease until adulthood. We conclude that the temporal and spatial pattern of Nb1 expression coincides with late stages of embryonic development, suggesting that it plays a role in regulating neuronal morphology and migration.

### *Perturbation of Neurabin-I Signaling In Vitro Affects Neuronal Morphology*

To test the involvement of Nb1 during early stages of neuronal differentiation, we examined the consequences of Nb1 overexpression in rat embryonic hippocampal neurons. We observed that 24 h after transfection, increased levels of Nb1 caused a decrease in neuronal complexity when compared with GFP-expressing controls (Figure 2A). Thus on average Nb1-overexpressing neurons exhibited a 28% reduction in total neurite length (Figure 2B; $p < 0.001$) and a 21% reduction in the number of neurites (Figure 2C; $p < 0.001$; $n > 200$ neurons from three different experiments for each condition). The DNA vector we used enabled GFP coexpression with Nb1 from an internal ribosome entry site (IRES) sequence, allowing us to easily distinguish neurons with different levels of Nb1. We found that the severity of the morphological consequences, particularly inhibition of neurite outgrowth, correlated with the degree of Nb1 overexpression. Thus, higher levels of Nb1 resulted in the elaboration of shorter neurites (Supplementary Figure 1A).

After 3 d in culture most control neurons expressing only GFP had polarized, forming one longest neurite that we considered the future axon and several shorter dendrites. At this stage Nb1 overexpression continued to cause reduced neurite outgrowth, although to a lesser degree than observed after 24 h in culture (compare a 28% reduction after 24 h with 18% after 3 d in culture). Significantly, the degree of outgrowth was reduced to a similar extent in all neurites (the longest neurite was reduced by 19% in comparison to an 18% reduction in outgrowth of all other neurites), indicating that Nb1 overexpression did not differentially affect the future axon. No differences were observed in the extent of neurite branching. These results suggest that increased levels of Nb1 primarily disrupt neurite outgrowth, rather than early stages of polarization.

To determine the long-term consequences of Nb1 overexpression, we examined neurons 7 d after transfection for the distribution of axonal (Tau-1) and dendritic (Map2) markers (Figure 2D). At this stage it was not possible to accurately determine neurite length because of the increased morphological complexities. After 7 d in culture most of the GFP-expressing controls had polarized with only 22 ± 2% elaborating more than one axon. In contrast, 38 ± 4% of Nb1-expressing neurons showed more than one Tau-1–positive axon (Figure 2E; $p < 0.05$; $n > 400$ neurons from four different experiments for each condition). The average number of Tau-1–positive processes per neuron increased upon Nb1 overexpression from 1.27 ± 0.03 (seen in GFP controls) to 1.52 ± 0.05 (Figure 2F; $p < 0.001$). Enrichment of Map2 confirmed the identity of the Tau-1–negative dendrites. The uniform consequences of Nb1 overexpression on neurite outgrowth, coupled with the fact that only a fraction of neurons had multiple axons, lead us to propose that Nb1 affects polarity indirectly, as a consequence of its regulation of neuronal morphology.

To test the consequence of Nb1 down-regulation in developing neurons, we designed two shRNA expression vectors targeting unique noncoding regions of the *nb1* mRNA and compared them to a scrambled control shRNA. Their ability to reduce Nb1 protein levels was confirmed by Western blot of transfected cortical neurons after 3 d in culture (Figure 3I). Morphological analyses of transfected neurons after 24 h in culture revealed that expression of control shRNA had no effect, with neurons displaying classical stage 2 and stage 3 morphologies (Figure 3, A and B). In contrast, even at this early time point, neurons expressing either sh1 or sh2 displayed broader cell bodies and extended very short and wide neurites that terminated in splayed growth cones (Figure 3, C–F). In all cases the increased lamellipodia were rich in F-actin. F-actin was also observed in filopodia-like spiked structures seen on the sides and termini of most neurites

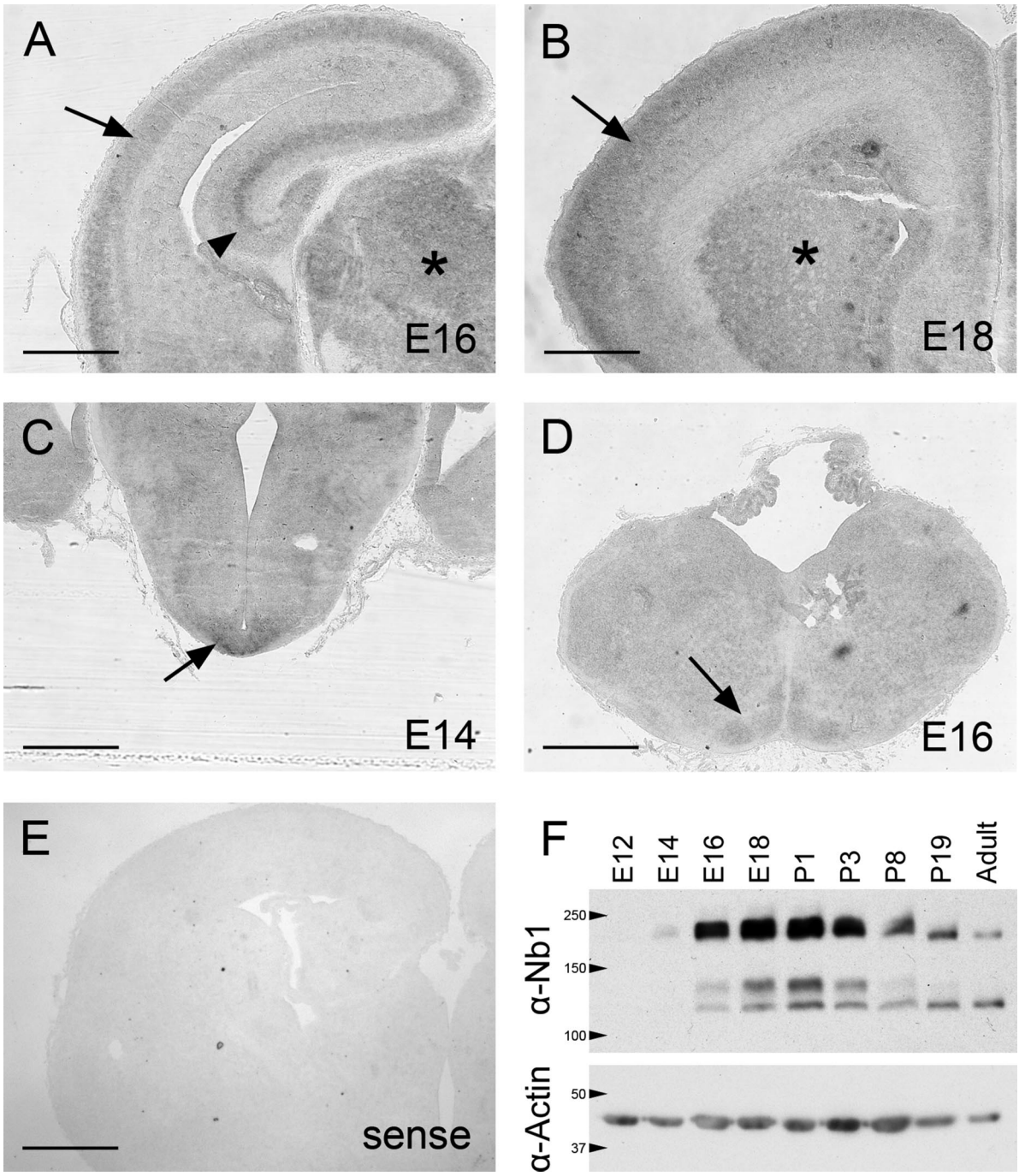


**Figure 1.** Nb1 expression in the developing brain. (A–D) In situ hybridization revealed a basal level of *nb1* mRNA expression throughout the brain (compare with the sense probe shown in E). (A and B) Highest *nb1* expression was observed in the cortical plate (arrow), hippocampus (arrowhead), and thalamus (asterisk) at E16 (A) and E18 (B). (C) Enrichment of *nb1* transcripts in the hypothalamus was observed from E14 (arrow) and is maintained throughout development (not shown). (D) *Nb1* expression in the inferior olive at E16 (arrow). (E) Control experiment using a sense probe revealing a complete absence of staining. (F) Western blot illustrating the expression of Nb1 during brain development. Nb1 is undetectable at E12, and only low levels are evident at E14. From E16, expression dramatically increases to reach a peak at E18–P1. Nb1 levels subsequently decrease and are low in adulthood. Detection of α-actin was used as a control for equal loading (bottom panel). Size bars, (A–E) 400 $\mu$m.

(Figure 3, D–F, and Supplementary Figure 1B). Total neurite length was reduced by 25 or 23%, after expression of sh1 or sh2, respectively (Figure 3G; $p < 0.001$; $n > 250$ neurons from three different experiments for each condition). Furthermore, an 18% decrease in the number of neurites per neuron was observed after Nb1 down-regulation (Figure 3H; $p < 0.001$). Significantly, a correlation was observed between the severity of the phenotype and the levels of sh1 and sh2 expression. Thus neurons with highest GFP immunoreactivity, and therefore lowest levels of Nb1, displayed the most disrupted morphologies and reduced neurite outgrowth (Supplementary Figure 1B). In all cases neuronal

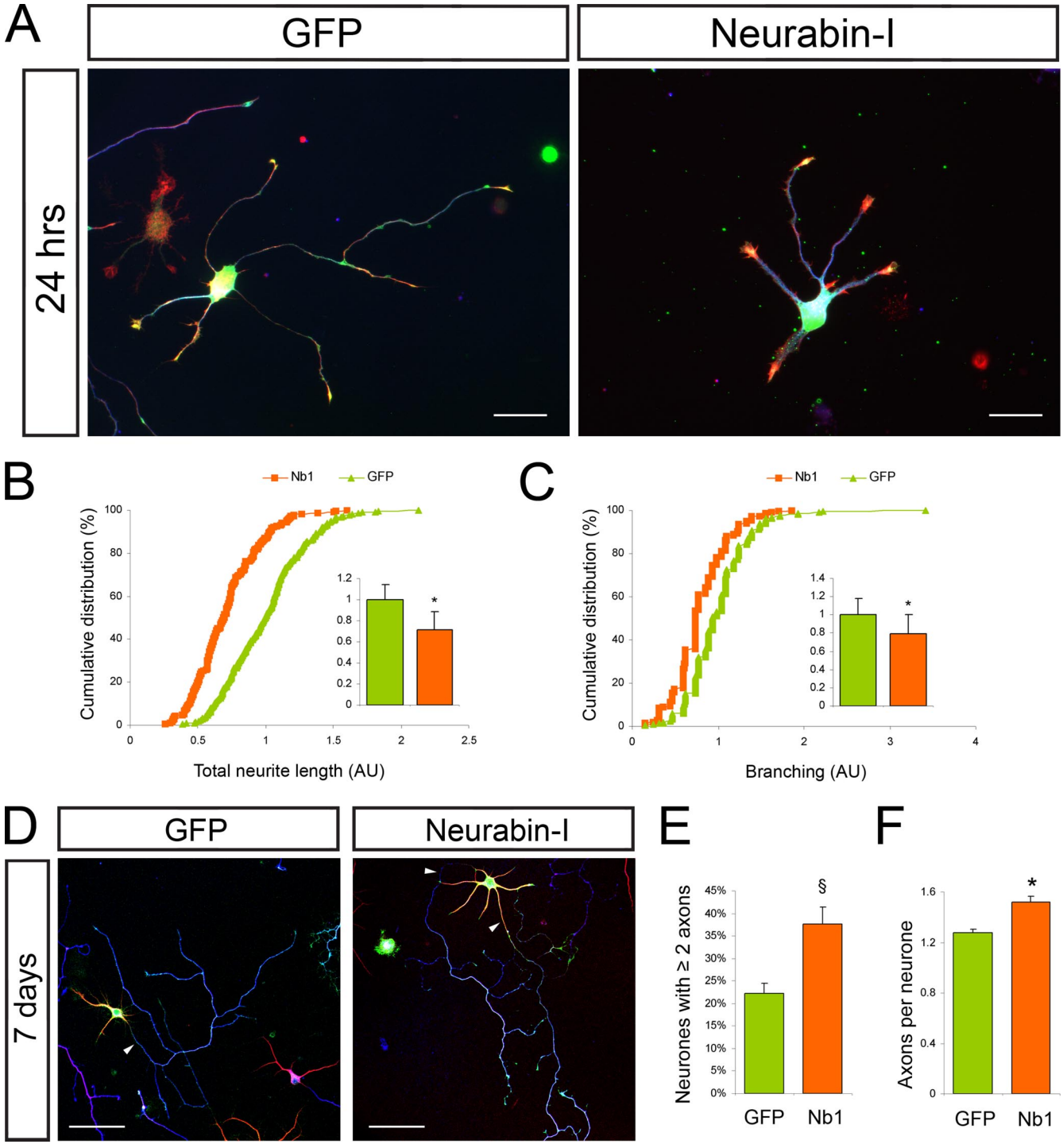


**Figure 2.** Nb1 overexpression affects neuronal morphology. Dissociated hippocampal neurons were transfected before plating and fixed after 24 h or 7 d in culture. (A) Neurons were stained for GFP (green), F-actin (red), and tubulin (TUJ1, blue). Nb1-overexpressing neurons exhibited simplified morphologies compared with GFP-expressing controls. Quantification of (B) total neurite length and (C) number of branches per neuron (expressed in arbitrary units and normalized to 1 in control conditions) are represented as cumulative distributions and histograms (mean ± SEM; $n > 200$ neurons taken from three different experiments for each condition; *$p < 0.001$). After 7 d in culture (D) axonal specification was assessed after Tau-1 (blue), Map2 (red), and GFP (green) staining. Arrowheads indicate Tau-1–positive axons. (E) Nb1 transfection resulted in an increased percentage of neurons showing two or more Tau-1–positive processes ($n = 4$ experiments; §$p < 0.05$). (F) Histogram representing the average number of Tau-1–positive processes per neuron ($n > 400$ neurons from four experiments; *$p < 0.001$). Size bars, (A) 25 μm; (D) 50 μm.

identity was confirmed by immunoreactivity for the neuron specific marker β-III-tubulin (TUJ1). Down-regulation of Nb1 continued to affect neuronal morphology and neurite outgrowth after 3 d in culture in a manner similar to that

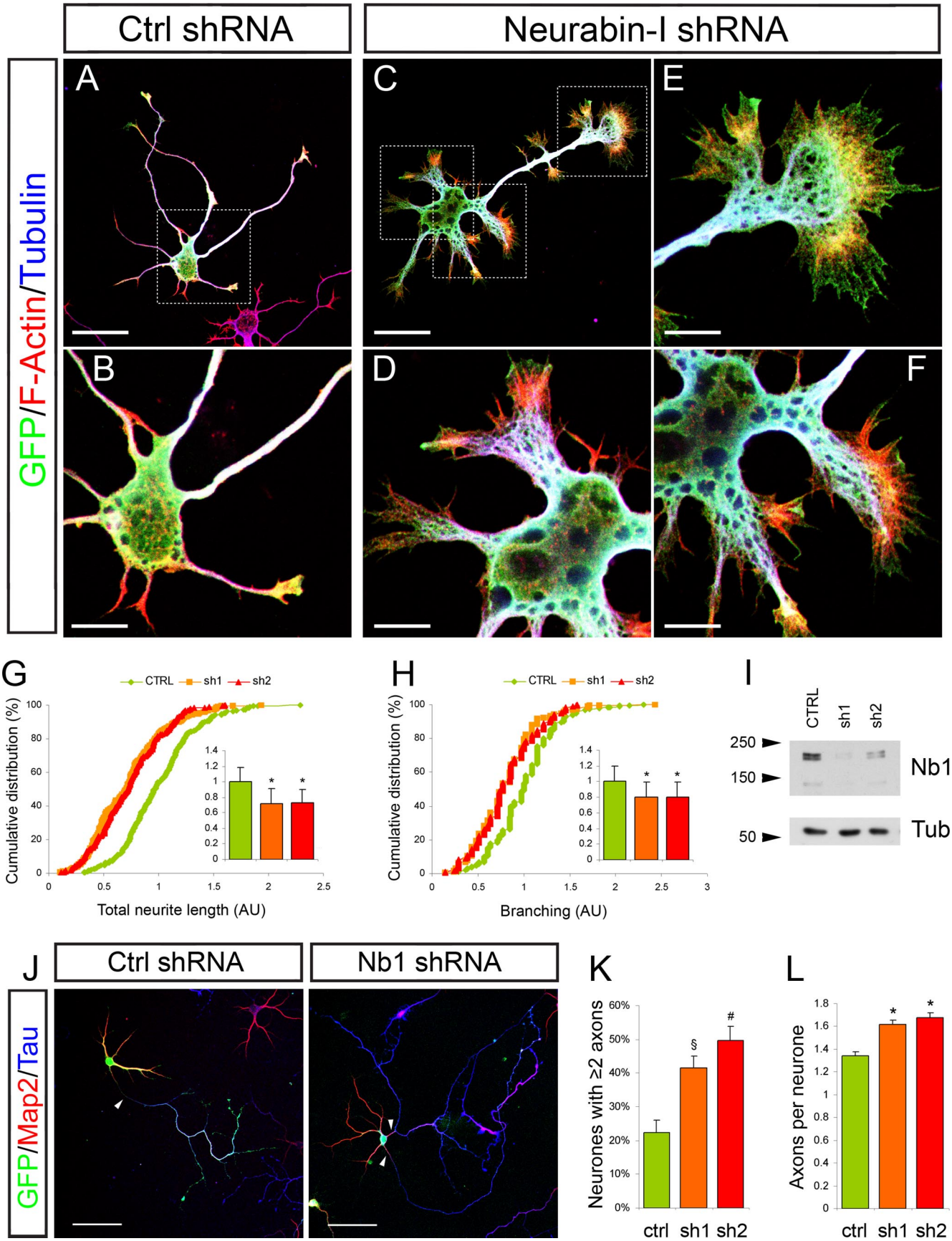
Ctrl shRNA
Neurabin-I shRNA
GFP/F-Actin/Tubulin
A
B
C
D
E
F
G
CTRL
sh1
sh2
Cumulative distribution (%)
Total neurite length (AU)
H
Branching (AU)
I
CTRL
sh1
sh2
250
150
50
Nb1
Tub
J
Ctrl shRNA
Nb1 shRNA
GFP/Map2/Tau
K
Neurones with ≥2 axons
ctrl
sh1
sh2
L
Axons per neurone

**Figure 3.**

seen after 24 h. Prolonged loss of Nb1 further increased the degree of F-actin rearrangement, particularly the incidence of spiked structures, the extent of which correlated with the degree of Nb1 down-regulation (Supplementary Figure 1, C–E).

After 7 d in culture, reduction of Nb1 levels increased the frequency of Tau-1–positive neurites, with 41 ± 4% ($p < 0.05$) of neurons expressing sh1 and 49 ± 4% ($p < 0.01$) expressing sh2 elaborating more than one Tau-1–positive neurite, in contrast to 22 ± 4% of the controls (Figure 3, J and K; n >300 neurons from three experiments for each condition). The average number of Tau-1–positive processes per neuron increased from 1.34 ± 0.04 in controls to 1.61 ± 0.05 or 1.67 ± 0.04 after transfection with sh1 or sh2, respectively (Figure 3L; $p < 0.001$). Together, our results indicate that Nb1 is required in vitro for the establishment of correct neuronal morphology. Interestingly, both overexpression and down-regulation of Nb1 have overlapping consequences on neurite outgrowth, suggesting that precise regulation of its levels is essential for neuronal differentiation. It is important to note that crucial morphological differences are also apparent between the consequences of upregulation or down-regulation of Nb1 levels. This is most clearly evident with the induction of F-actin–rich protrusions, the prevalence of which correlates with the degree of Nb1 reduction.

### *Perturbation of Neurabin-I Signaling Affects Neocortical Migration In Vivo*

The mammalian cerebral cortex develops in a highly ordered manner with early born neurons taking up positions deep within the cortical plate and late born neurons residing in peripheral regions, closer to the pial surface. Because the timing of layer formation is well established in mice, the developing cerebral cortex is an ideal system to study the role of proteins that are implicated in controlling neuronal movement and morphology. To examine the role of Nb1 in vivo, we used in utero electroporation of E14.5 murine cortical precursors as a means to interfere with endogenous Nb1 signaling and examine the consequences in a physiological environment. Embryos were allowed to develop until birth (P0) when the position and morphology of the targeted neurons was analyzed. We subdivided the cortex into three zones using DAPI and MAP2 staining as references: 1) the superficial cortical plate corresponding to layers II–IV, where neurons that were labeled at E14.5 should normally reside at P0; 2) the deep cortical plate corresponding to layers V and VI, formed by neurons that had completed their migration during earlier stages of corticogenesis; and 3) the intermediate zone (IZ), localized immediately beneath the cortical plate (Figure 4A). The ventricular/subventricular zones (VZ/SVZ) were not examined because the identity of the cells localized in these regions is difficult to assess. Furthermore, the presence of GFP-positive cells in the VZ/SVZ is affected by the proximity of the site of electroporation, which complicates scoring.

At birth the majority of control GFP-transfected neurons (85 ± 4%) were localized at the periphery in layers II–IV, and only 10 ± 2% were seen in layers V–VI and 5 ± 2% in the IZ (Figure 4, A and B). This corresponded well with the normal pattern of neuronal migration. Interestingly, overexpression of Nb1 caused a reduction in the number of neurons residing in the superficial layers with only 52 ± 3% detected in layers II–IV, whereas 32 ± 2% remained in layers V–VI and 16 ± 1% in the IZ ($p < 0.001$ in layers II–IV and V–VI, $p < 0.01$ in the IZ; GFP, n = 4; Nb1, n = 5). To further understand the consequences of Nb1 overexpression, we analyzed the morphologies of the targeted neurons. The few GFP-positive controls that were evident in the IZ had oriented an often ruffled leading process toward the pial surface, suggestive of their migratory route toward the cortical periphery. Neurons overexpressing Nb1 in the IZ were indistinguishable from the GFP-expressing controls. Their correct orientation toward the pial surface indicated normal polarization. Both the controls and Nb1-overexpressing neurons that were evident in deep cortical layers (V–VI) had clear bipolar morphologies characteristic of migrating neurons. However, neurons with increased Nb1 levels commonly elaborated defective protrusions. These morphological alterations included reduced length and thickening and branching of the leading and lagging processes (Figure 4C). At the cortical periphery, the most apparent feature of electroporated neurons were the elaborate apical dendrites, whereas the axons were obscured because of the large number of fluorescent fibers. Neurons with increased levels of Nb1 elaborated dendrites that appeared similar to those seen in the controls, suggesting the absence of any major defects (Figure 4D). Together our results indicate that in vivo Nb1 overexpression affects neuronal morphology, which is most apparent in migrating neurons. Importantly, the correct orientation of migrating neurons and the dorsal position of apical dendrites indicate that increased levels of Nb1 did not directly affect polarization. The fact that at P0 more Nb1-overexpressing neurons were evident in the deep cortical layers than the IZ, coupled with their often branched morphologies, indicates a delayed rather than arrested motility.

To examine the consequences of loss of Nb1 function, we electroporated mouse E14.5 cortices with the shRNA expression vectors. In utero electroporation with control shRNA resulted in 77 ± 4% of the transfected neurons reaching the superficial layers (II–IV), whereas only 4 ± 2% remained in the IZ. Their distribution and morphology was indistinguishable from GFP-expressing controls, confirming the neutral consequences of control shRNA expression (Figure 5A). In contrast, Nb1 knockdown using sh1 or sh2 resulted in a strong perturbation of the migratory behavior, with 35 ± 5 and 31 ± 4%, respectively, residing in the IZ. Inter-

**Figure 3 (facing page).** Nb1 down-regulation affects neuronal morphology. Dissociated hippocampal neurons were cotransfected with GFP- and shRNA-expressing plasmids, and their morphology was analyzed 24 h after GFP (green), F-actin (red), and tubulin (TUJ1, blue) staining (A–F). Neurons transfected with a control shRNA (A, magnified view in B) were compared with neurons expressing shRNAs targeting Nb1 (C, magnified views in D–F). The latter often exhibited splayed soma and/or growth cones. (G) Quantification of total neurite length and (H) number of branches per neuron (expressed in arbitrary units and normalized to 1 in control conditions) are represented as cumulative distributions and histograms (mean ± SEM). Statistical analyses were performed using >250 neurons taken from three different experiments for each condition; *$p < 0.001$. (I) Cortical neurons were transfected with shRNA constructs, as shown. The relative amount of Nb1 in the lysates was assessed by Western blotting. α-Tubulin (lower panel) was used as a loading control. (J) Axonal specification was assessed after 7 d in culture after Tau-1 (blue), Map2 (red), and GFP (green) staining. Arrowheads indicate Tau-1–positive axons. (K) Down-regulation of Nb1 with sh1 or sh2 resulted in an increased percentage of neurons showing two or more Tau-1–positive processes (n = 3 experiments; §$p < 0.05$, #$p < 0.01$). (L) Histogram representing the average number of Tau-1–positive processes measured for each neuron (n > 300 neurons from three experiments; *$p < 0.001$). Size bars, (A and C) 30 μm; (B and D–F) 10 μm; (J) 50 μm.

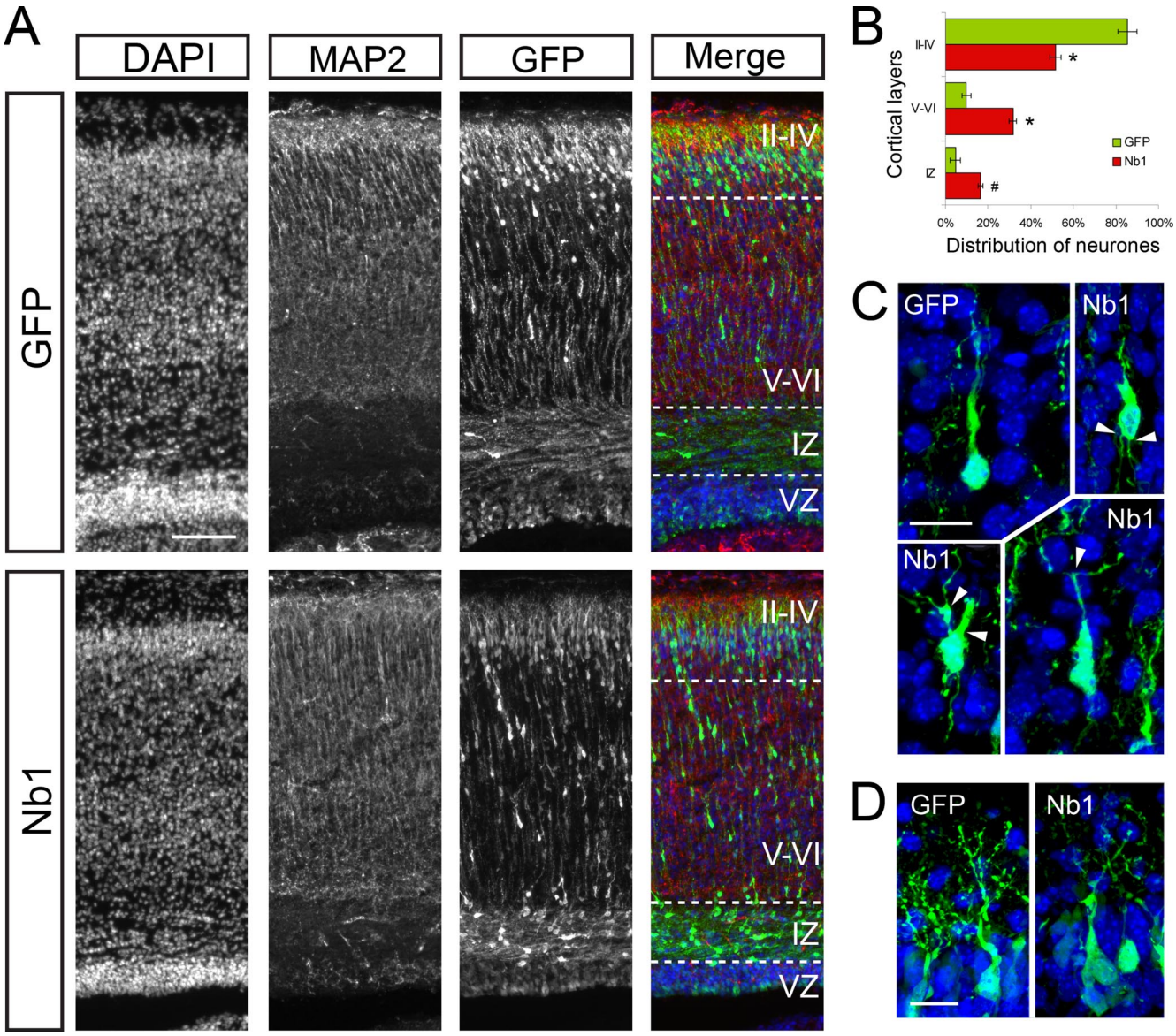


**Figure 4.** Nb1 overexpression affects neuronal migration in vivo. (A) GFP or Nb1 expression constructs were electroporated in utero in the cortical ventricular zone of E14.5 mouse embryos. Animals were fixed at P0, brains were dissected, and cryosections were prepared. DAPI staining allowed visualization of cell nuclei, MAP2 staining marked the cortical plate, and GFP staining revealed transfected cells. (B) GFP-positive cells were counted in the upper layers (II–IV), deeper layers (V–VI), and intermediate zone (IZ). The ventricular zone (VZ) was not taken into account. More than 10,000 cells were counted from n = 4 and 5 animals (for GFP and Nb1 transfections, respectively). Statistical analysis revealed that Nb1 overexpression significantly impairs migration (*$p < 0.001$; #$p < 0.01$). (C) Comparison of the morphologies of neurons localized in layers V–VI revealed that Nb1 overexpression induces the formation of supernumerary or branched processes (arrowheads). (D) Neurons overexpressing Nb1 or GFP that reached layers II-IV formed apical dendrites that appeared indistinguishable. Size bars, (A) 100 $\mu$m; (C) 15 $\mu$m; (D) 10 $\mu$m. All images are presented in pial surface, Up, and basal (ventricular), Down, orientation.

estingly, few neurons were found in layers V–VI; thus, 50 ± 6% of sh1- and 49 ± 4% of sh2-transfected neurons reached layers II–IV ($p < 0.05$ and $p < 0.01$, respectively; n = 3 animals in each condition; Figure 5, A and B). The sh1/sh2 expressing neurons located in the IZ often accumulated at the upper limit of the IZ, suggesting that they were not able to migrate into the cortical plate (CP). Close examination of the targeted neurons revealed highly simplified morphologies. In the IZ cell protrusions were thinner and often disoriented (Figure 5D). In deep cortical layers the few apparently migrating neurons had shorter, more splayed, and sometimes branched leading and lagging process (Figure 5C). In layers II–IV neurons with reduced Nb1 expression elaborated apical dendrites that appeared less complex than in controls (Figure 5E). We were able to correlate the severity of the migration defects with the degree of Nb1 down-regulation. Thus neurons that had migrated to the cortical periphery (layers II–IV) on average had 60% lower levels of GFP (and thus were more likely to express some Nb1) than those that had arrested in the IZ (Figure 5F; $p < 0.001$).

Taken together, our results confirm that gain and loss of Nb1 function in vivo affect the morphology and movement of migratory neurons. The fact that loss of Nb1 expression causes many neurons to arrest before entering the cortical plate indicates that in vivo Nb1 is required for regulated changes in neuronal morphology that are essential for motility.

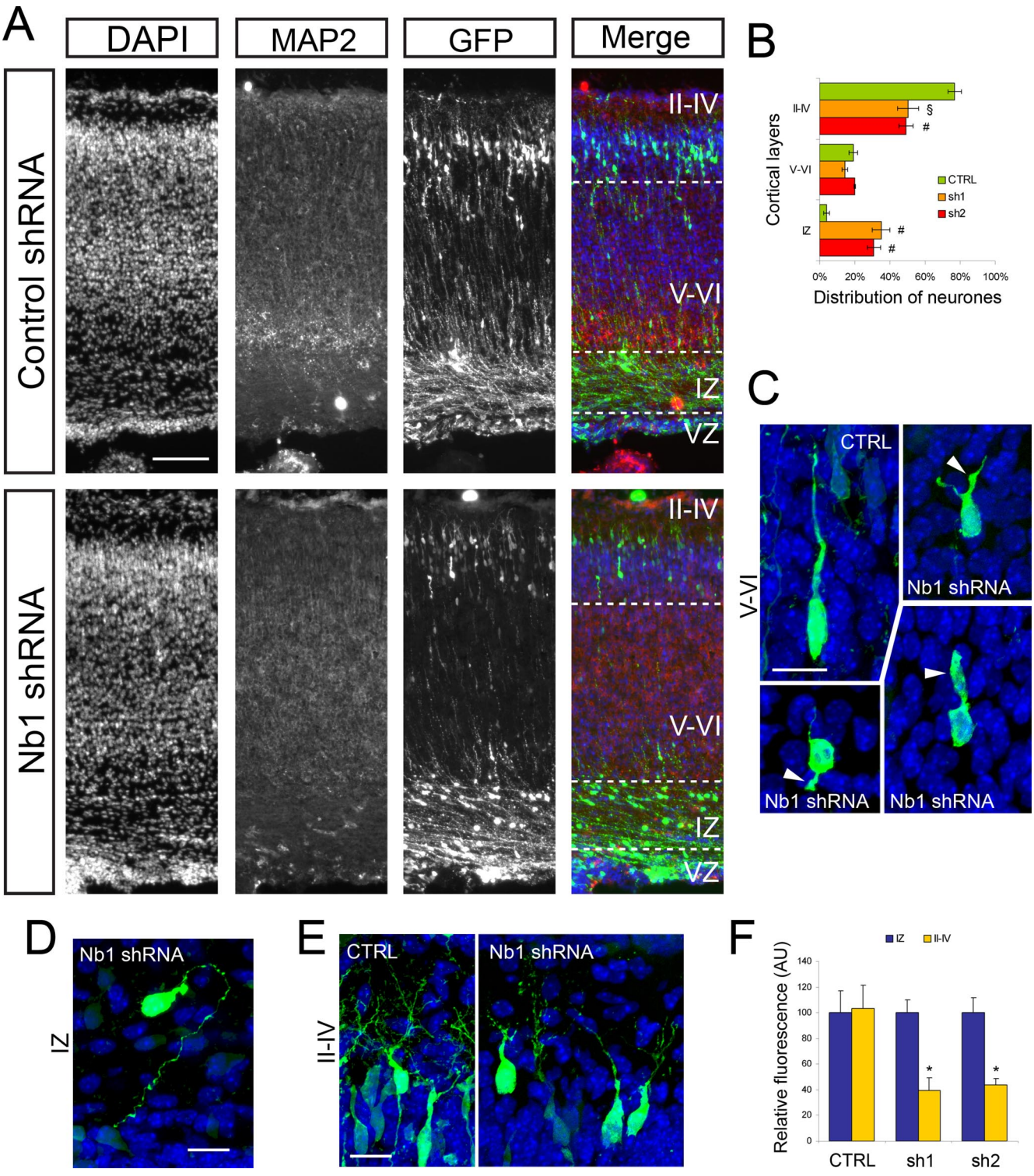


**Figure 5.** Nb1 down-regulation affects neuronal migration in vivo. (A) Control shRNA (CTRL) or Nb1-targeting shRNA constructs were coelectroporated with GFP in the cortical ventricular zone of E14.5 mouse embryos. Animals were fixed at P0, brains were dissected, and cryosections were prepared. DAPI staining allowed visualization of cell nuclei, MAP2 staining marked the cortical plate, and GFP staining revealed transfected cells. (B) GFP-positive cells were counted in the upper layers (II-IV), deeper layers (V–VI), and intermediate zone (IZ). The ventricular zone (VZ) was not taken into account. More than 4000 cells were counted from n = 3 animals for each shRNA construct. Statistical analysis revealed that down-regulation of Nb1 significantly impairs migration ($^{\#}p < 0.01$; $^{\S}p < 0.05$). (C) Comparison of the morphologies of neurons localized in layers V–VI revealed that Nb1 down-regulation induces the formation of shortened and thickened processes (arrowheads). (D) Neurons expressing Nb1 shRNA found in the IZ often exhibited misoriented leading processes. (E) The apical dendrites formed by neurons residing in layers II–IV appeared less complex after Nb1 down-regulation. (F) Quantification of the relative GFP fluorescence of cells located in the IZ and layers II–IV. Neurons expressing sh1/sh2 located in layers II–IV appeared on average ~60% less bright than their counterpart located in the IZ. Size bars, (A) 100 $\mu$m; (C–E) 15 $\mu$m. All images are presented in pial surface, Up, and basal (ventricular), Down orientation.

### *Neurabin-I Is Targeted by Cdk5*

The Cdk5 kinase plays an essential role in controlling neuronal morphology and migration in the developing cerebral cortex, two processes we have shown to require Nb1 signaling. Furthermore, the ability of Nb1 to associate with specific binding partners can be regulated by phosphorylation. Thus protein kinase A (PKA) inhibits the association between Nb1 and PP1 by phosphorylating Nb1 on S461 (McAvoy *et al.*, 1999). We therefore examined the Nb1 amino acid sequence for Cdk5 consensus sites (S/T-P-X-K/R; Songyang *et al.*, 1996) using the Scansite database (Obenauer *et al.*, 2003; http://scansite.mit.edu/). The highest score was obtained for a serine residue in position 95 (S95), which lies in the actin-binding domain of Nb1 (amino acids 1-144; Nakanishi *et al.*, 1997; see Figure 6A). To examine whether Cdk5 can phosphorylate S95, we performed in vitro kinase assays using a GST-fused Nb1 fragment (GST-Nb$^{1\text{-}144}$) as a substrate. On incubation with recombinant Cdk5 and its activator p35, GST-Nb1$^{1\text{-}144}$ incorporated radioactive phosphate, indicating that it is indeed phosphorylated by Cdk5 (Figure 6B). To assess that the phosphorylation actually occurs on S95, we designed a mutated unphosphorylatable version of Nb1$^{1\text{-}144}$ in which S95 was substituted by an alanine residue (GST-Nb1A95$^{1\text{-}144}$). In vitro phosphorylation of GST-Nb1A95$^{1\text{-}144}$ was greatly reduced indicating that Nb1 phosphorylation by Cdk5 occurs on S95 (Figure 6B). Nb1 bears a second Cdk5 consensus site in its actin-binding domain (S17), which is conserved in Neurabin-II/Spinophilin. Interestingly, Neurabin-II/Spinophilin was recently shown to be targeted by Cdk5 on S17, although no biological consequences were elucidated (Futter *et al.*, 2005). The Scansite database attributes a much lower score to S17 than to S95; however, we decided to test whether Cdk5 can also target Nb1 on S17. In contrast to the A95 mutant, removal of S17 did not affect the ability of Cdk5 to phosphorylate Nb1 in vitro, suggesting that it does not target S17 (Figure 6B).

To study the phosphorylation of Nb1 in a physiological environment, we raised an antibody directed against a peptide mimicking phospho-S95 Nb1 (pS95 Nb1; see *Materials and Methods* for details). The specificity of the antibody (subsequently referred to as anti-pS95Nb1) was confirmed by Western blot of lysates obtained from Cos7 cells coexpressing Cdk5, p35, and the full-length wild-type or A95-mutated Nb1. Nb1 phosphorylation on S95 was only detected in the presence of Cdk5 and p35. In contrast, Cdk5 did not phosphorylate the Nb1A95 mutant (Figure 6C). Taken together, these results demonstrate that p35/Cdk5 is sufficient for S95 phosphorylation of full-length Nb1 in a cellular environment.

### *Neurabin-I Is an In Vivo Substrate of Cdk5*

Cos7 cells do not endogenously express Nb1 or p35; therefore we examined the phosphorylation of Nb1 in primary neurons to reflect true in vivo signaling pathways. Significant levels of endogenous pS95 Nb1 were evident in E18 rat brain lysates, indicating its presence in the developing brain (Figure 6C) Exposure of cortical neurons to a Cdk5 inhibitor, roscovitine, caused a marked reduction of phosphorylation after down-regulation of Cdk5 activity, whereas the total amount of Nb1 remained unchanged (Figure 6D). We also compared the phosphorylation of Nb1 in wild-type and *cdk5*$^{-/-}$ mouse embryo brain lysates, revealing a dramatic reduction of pS95 Nb1 levels in the absence of Cdk5 (Figure 6E). Taken together, these results show that Nb1 is phosphorylated on S95 in the developing brain and that the Cdk5 kinase activity is necessary for this event to occur.

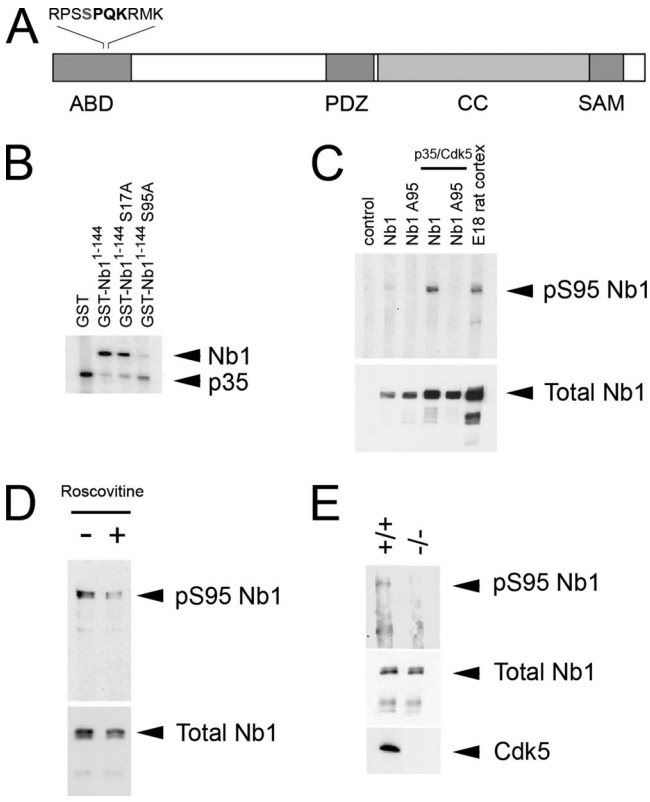


**Figure 6.** Nb1 is phosphorylated by p35/Cdk5. (A) Nb1 contains an actin-binding domain (ABD), a PSD-95/Dlg/ZO-1 (PDZ) domain, a coiled-coiled (CC) domain, and a sterile alpha motif (SAM). S95 (in grey) lies in the ABD, in a perfect consensus for the Cdk5 kinase (represented in bold). (B) Kinase assay demonstrating in vitro phosphorylation of Nb1 by p35/Cdk5. The higher band corresponds to GST-Nb1$^{1\text{-}144}$ and denotes radioactive phosphate incorporation. The lower band corresponds to p35 phosphorylation. A S95A mutation almost completely abolishes GST-Nb1$^{1\text{-}144}$ phosphorylation by p35/Cdk5. (C) Cos7 cells expressing full-length Nb1 (wild type or A95 mutated) in the presence or absence of p35/Cdk5. Cells were lysed, and the obtained extracts were subjected to immunoprecipitation with an anti-Nb1 antibody followed by Western blotting with either anti-pS95 Nb1 (top panel) or anti-Nb1 (bottom panel). E18 rat cortex lysates were used as a positive control. S95-phosphorylated Nb1 could only be detected in cells transfected with wild-type Nb1 and p35/Cdk5 as well as in brain extracts. (D) Cortical neurons were cultured for 48 h in the presence (+) or absence (−) of 10 $\mu$M of the Cdk5 inhibitor, roscovitine. Immunoprecipitation with an anti-Nb1 antibody followed by Western blotting with either anti-pS95 Nb1 (top panel) or anti-Nb1 (bottom panel) revealed a decrease in Nb1 S95-phosphorylation after drug treatment. (E) Brain extracts from wild-type (+/+) or *cdk5*-deficient (−/−) mice were subjected to immunoprecipitation with an anti-Nb1 antibody followed by Western blotting with either anti-pS95 Nb1 (top panel) or anti-Nb1 (middle panel). We failed to detect significant levels of S95-phosphorylated Nb1 in *cdk5*$^{-/-}$ brains. A cdk5 Western blot (bottom panel) confirmed the genotype of *cdk5*-deficient mice.

### *Phosphorylation of Neurabin-I Affects Its Ability to Bind F-Actin*

Actin-binding is an essential feature of Nb1 function (Oliver *et al.*, 2002); we therefore tested the hypothesis that Cdk5 regulates the association between Nb1 and F-actin through phosphorylation of the latter on S95. We subjected recombinant GST-Nb1$^{1\text{-}144}$ (both wild-type and the unphosphorylatable A95 mutant) to in vitro phosphorylation in the presence of p35/Cdk5. The efficiency of the reaction was assessed through Western blot using the anti-pS95Nb1 antibody (Figure 7B). The

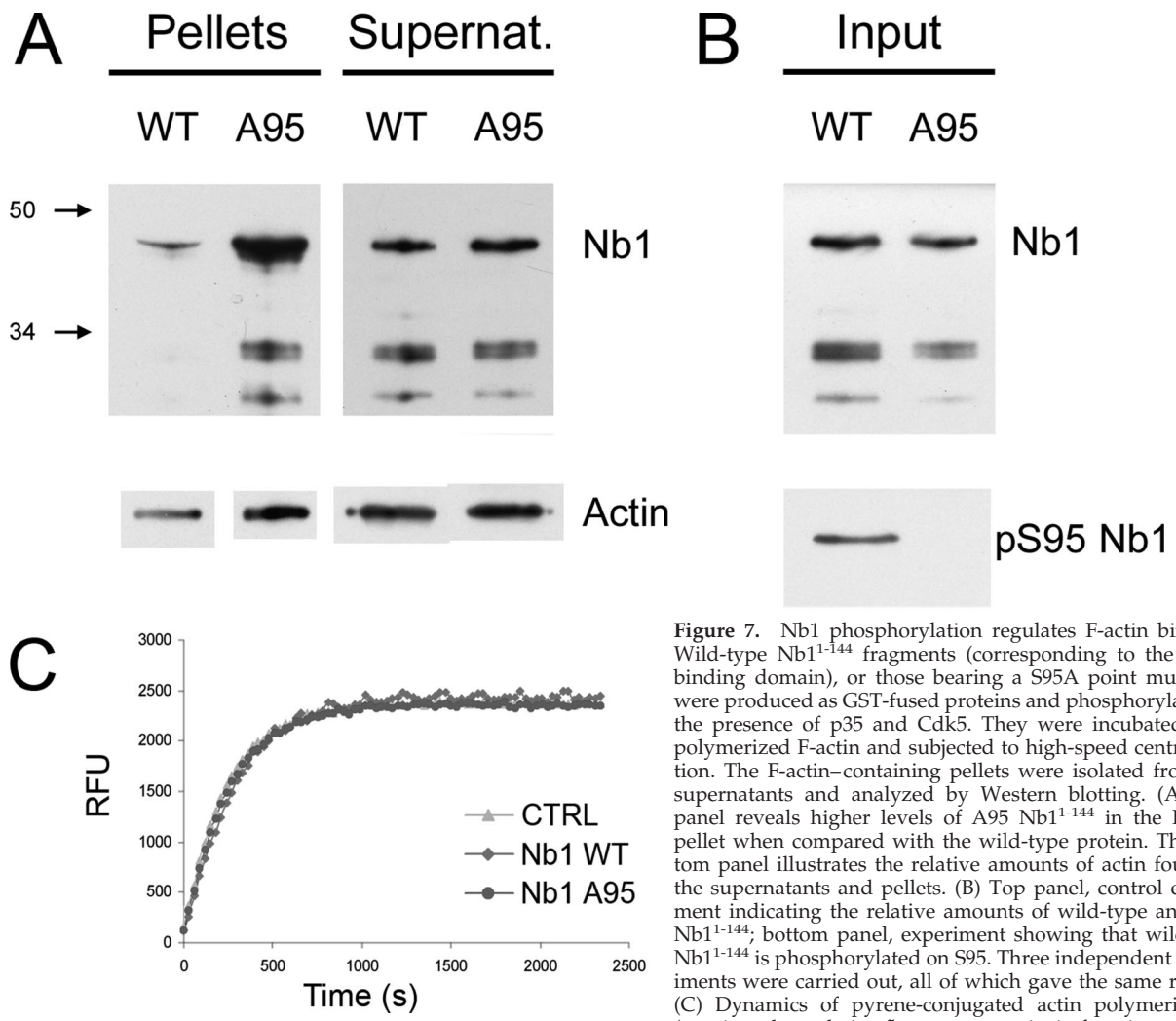


**Figure 7.** Nb1 phosphorylation regulates F-actin binding. Wild-type $Nb1^{1-144}$ fragments (corresponding to the actin-binding domain), or those bearing a S95A point mutation, were produced as GST-fused proteins and phosphorylated in the presence of p35 and Cdk5. They were incubated with polymerized F-actin and subjected to high-speed centrifugation. The F-actin–containing pellets were isolated from the supernatants and analyzed by Western blotting. (A) Top panel reveals higher levels of A95 $Nb1^{1-144}$ in the F-actin pellet when compared with the wild-type protein. The bottom panel illustrates the relative amounts of actin found in the supernatants and pellets. (B) Top panel, control experiment indicating the relative amounts of wild-type and A95 $Nb1^{1-144}$; bottom panel, experiment showing that wild-type $Nb1^{1-144}$ is phosphorylated on S95. Three independent experiments were carried out, all of which gave the same results. (C) Dynamics of pyrene-conjugated actin polymerization (monitored as relative fluorescence units in function of time) indicates that the presence of Nb1 (phosphorylated or not) neither affects the rate of polymerization nor the F/G-actin ratio once the plateau is reached.

fragments were subsequently incubated with polymerized F-actin filaments, and the amount of GST-$Nb1^{1-144}$ bound to F-actin was assessed after precipitation by high-speed centrifugation. A similar approach was previously taken to demonstrate the ability of the GST-$Nb1^{1-144}$ fragment to cosediment with F-actin (Oliver *et al.*, 2002). We found that after preincubation with active Cdk5, the amount of Nb1 that cosedimented with F-actin was greatly reduced compared with the nonphosphorylatable A95 mutant. (Figure 7A; identical results were obtained in three independent experiments). Control experiments in which the phosphorylation step was omitted revealed that both the wild-type and A95 forms of GST-$Nb1^{1-144}$ share the same F-actin–binding properties (not shown). This is a critical point as it demonstrates that the S-to-A substitution itself does not affect the Nb1–F-actin interaction. To examine whether phosphorylation of Nb1 on S95 regulates the rate of actin polymerization, we incubated wild-type or A95 GST-$Nb1^{1-144}$, previously subjected to in vitro phosphorylation, with pyrene-conjugated actin. Polymerization was measured as an increase in fluorescence. No differences were observed indicating that Nb1 S95 phosphorylation does not influence actin polymerization or the F- and G-actin equilibrium (Figure 7C). We thus conclude that by phosphorylating Nb1 on S95, Cdk5 can regulate its ability to associate with actin filaments in vitro and may therefore be an important regulator of the functional relationship between Nb1 and F-actin.

### *Phosphorylation of Neurabin-I Controls Neuronal Morphology*

Nb1 has been proposed to act as a targeting subunit, localizing its numerous binding partners to the F-actin cytoskeleton. The possibility of Cdk5 regulating this function through phosphorylation is exciting but remains to be demonstrated in a physiological environment. To analyze the biological importance of S95 phosphorylation, we compared the consequences of Nb1 overexpression in hippocampal neurons, with those of the Nb1A95 mutant. After 24 h in culture, no differences were observed between neurons expressing Nb1 or Nb1A95 with respect to total neurite length and the number of neurites (not shown). However, morphological differences became apparent if the cultures were allowed to develop for 48 h when expression of wild-type Nb1 caused a 21% reduction in neurite outgrowth, compared with GFP-expressing controls ($p < 0.001$). Interestingly, neurons expressing Nb1A95 exhibited a milder phenotype, with only a 14% reduction in total neurite outgrowth

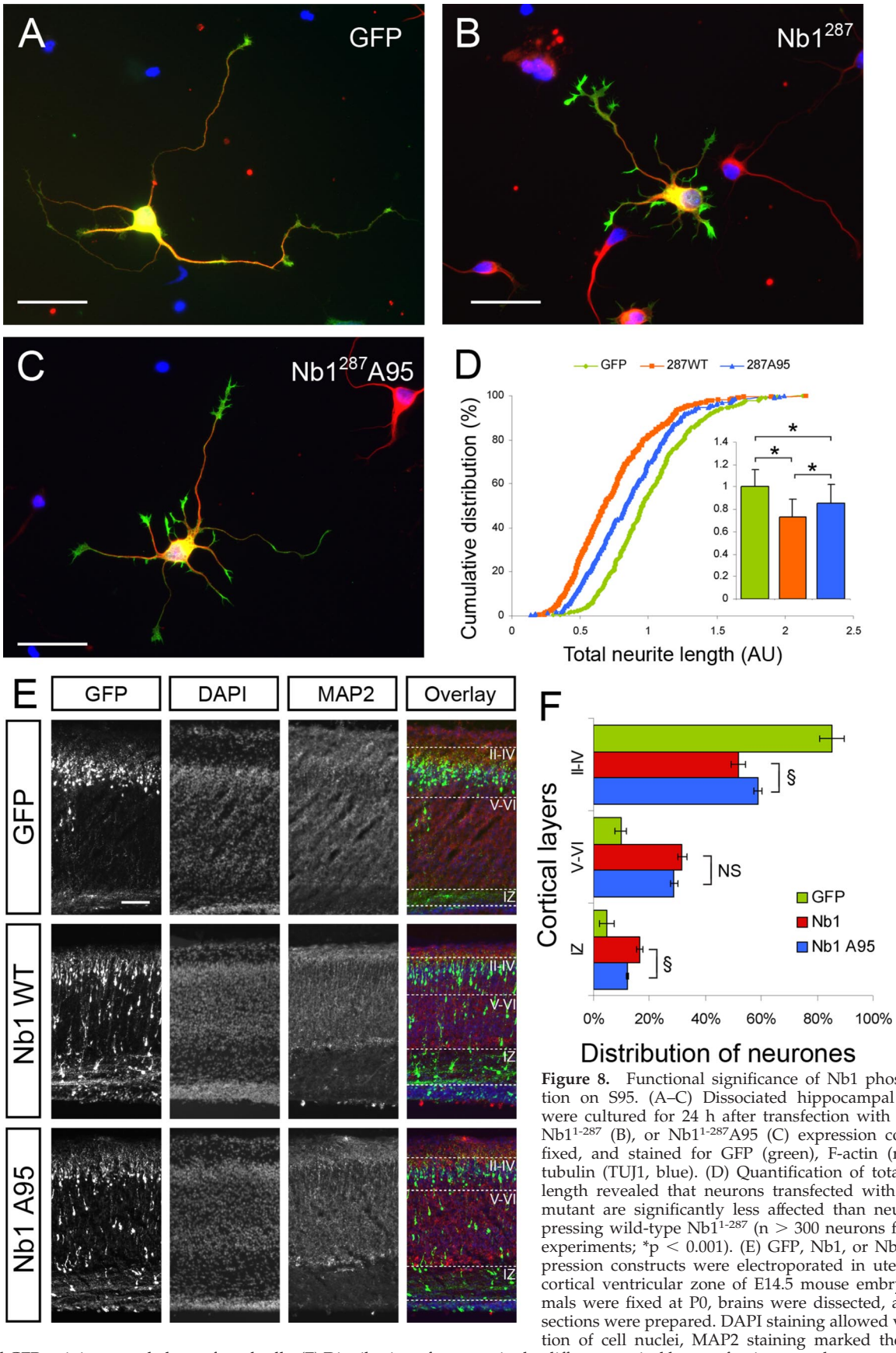


**Figure 8.** Functional significance of Nb1 phosphorylation on S95. (A–C) Dissociated hippocampal neurons were cultured for 24 h after transfection with GFP (A), $Nb1^{1-287}$ (B), or $Nb1^{1-287}$A95 (C) expression constructs, fixed, and stained for GFP (green), F-actin (red), and tubulin (TUJ1, blue). (D) Quantification of total neurite length revealed that neurons transfected with the A95 mutant are significantly less affected than neurons expressing wild-type $Nb1^{1-287}$ ($n > 300$ neurons from four experiments; *$p < 0.001$). (E) GFP, Nb1, or Nb1A95 expression constructs were electroporated in utero in the cortical ventricular zone of E14.5 mouse embryos. Animals were fixed at P0, brains were dissected, and cryosections were prepared. DAPI staining allowed visualization of cell nuclei, MAP2 staining marked the cortical plate, and GFP staining revealed transfected cells. (F) Distribution of neurons in the different cortical layers after in utero electroporation with GFP, wild-type, or A95 Nb1 (data collected from 4, 5, and 5 animals, respectively). Quantification of the proportion of neurons found in the

($p < 0.05$ compared with wild-type Nb1; $n > 200$ neurons from three experiments for each condition). To confirm this result, we tested the effect of a Nb1 truncation mutant (amino acids 1-287) previously shown to affect neuronal morphology more dramatically than the full-length protein (Zito *et al.*, 2004; Terry-Lorenzo *et al.*, 2005). Consistent with the previous reports, $Nb1^{1-287}$ increased the number and size of filopodia seen along the neurites (compare Figure 8, A and B). After 24 h in culture, expression of wild-type $Nb1^{1-287}$ resulted in a 26% reduction in total neurite length compared with GFP-expressing neurons (Figure 8, A–D; $p < 0.001$), whereas A95 $Nb1^{1-287}$ expression only resulted in a 14% decrease ($p < 0.001$ compared with GFP- expressing neurons and $p < 0.001$ compared with wild-type $Nb1^{1-287}$-expressing neurons; $n > 300$ neurons from four experiments for each condition). Together these results indicate that loss of Nb1 phosphorylation on S95 reduces the severity of its overexpression during neurite outgrowth.

To examine the biological role of S95 phosphorylation in vivo we performed in utero electroporations to introduce the Nb1A95 mutant into embryonic cortical progenitors. Similarly to our results in dissociated neuronal cultures, expression of the Nb1 A95 mutant in the developing cerebral cortex had milder effects than wild-type Nb1. Thus 59 ± 2% of Nb1A95-positive cells resided in layers II–IV (in contrast to 52 ± 3% of Nb1 and 85 ± 4% of GFP-expressing neurons), 29 ± 1% located to layers V–VI (in contrast to 32 ± 2% Nb1 and 10 ± 2% GFP) and 12 ± 1% were evident in the IZ (compared with 16 ± 1% Nb1 and 5 ± 2% GFP; Figures 4 and 8, E and F). Quantification indicated that the proportion of transfected neurons localized in the IZ significantly decreased after Nb1A95 electroporation compared with wild-type Nb1 (Figure 8F, $p < 0.05$), and the proportion in layers II-IV significantly increased (Figure 8E; $p < 0.05$). In contrast, no significant differences were observed in the proportion of neurons localized in layers V–VI. Altogether, these results suggest that part of the effects observed after Nb1 overexpression can be attributed to S95-phosphorylation of Nb1, highlighting the importance of the regulation by the Cdk5 kinase during developmental processes, particularly for the establishment of correct neuronal morphology and migration.

### *Neurabin-I Regulates Rac1 Activity in Neurons*

Nb1 can associate with two Rho GTPase GEFs, Kalirin, and Lfc (Penzes *et al.*, 2001; Ryan *et al.*, 2005). Although the functional significance of Nb1/Kalirin interactions are still uncertain, Nb1 was shown to mediate localized activation of RhoA by Lfc (Ryan *et al.*, 2005). Nb1 can also directly associate with Rac3 and modulate its ability to induce process outgrowth in neuronal cell lines (Orioli *et al.*, 2006). A number of studies have revealed the requirement for Rac1 in promoting neurite outgrowth (Luo, 2000; Lundquist, 2003); however to date it is not clear whether Nb1 can also regulate its function. Interestingly, Rac1 activity has been shown to control the subcellular distribution of Neurabin-II/Spinophilin (Stephens and Banting, 2000). Furthermore, Neurabin-II/Spinophilin can associate with the Rac1 specific GEF, Tiam-1, causing preferential activation of p70 S6 kinase over other Rac1 effectors such as the Pak1 kinase (Buchsbaum *et al.*, 2003). It is therefore clear that Nb1 and Neurabin-II/Spinophilin can regulate the temporal and spatial pattern of Rho GTPase activity and may also affect selective induction of specific downstream signaling pathways. Because we observed that changes in Nb1 expression affect neurite outgrowth and morphology, we examined the consequences on Rac1 activation. The levels of active (GTP-bound) endogenous Rac1 were compared between control cortical neurons and those expressing Nb1 shRNA or overexpressing Nb1. Interestingly, overexpression of Nb1 caused a ~40% reduction in the levels of GTP-bound Rac1. In contrast, expression of Nb1 shRNA induced Rac1 activity by ~70% (Figure 9, A and B). No differences were observed after expression of control shRNA when compared with nontransfected neurons (data not shown). The effects of Nb1 expression were confirmed in Cos7 cells where endogenous Rac1 was down-regulated to a similar degree as seen in primary neurons (Figure 9C). These experiments were carried out in the presence of the p35/Cdk5 kinase, thus mimicking neuronal signaling pathways. Interestingly, endogenous Rac1 specifically coimmunoprecipitated with Nb1, indicating that these two proteins associate or are found in the same signaling complex (Figure 9C). Together our results suggest that Nb1 may regulate neuronal morphology and migration at least in part by controlling the levels of active Rac1.

## DISCUSSION

We have shown that Nb1 plays an important role during embryonic brain development. Our finings confirm and expand on the previously reported role of Nb1 in controlling neurite outgrowth (Nakanishi *et al.*, 1997; Orioli *et al.*, 2006) by providing detailed effects of Nb1 loss and gain of function on neuronal morphology. Unexpectedly, we found that increases and reductions of Nb1 levels affected neurite outgrowth. However, the formation of lamellipodia and F-actin–rich spiked structures seen around the soma, at the tips, and along the length of neurites was only evident after down-regulation of Nb1. Interestingly, expression of the Nb1 F-actin–binding domain was previously shown to induce F-actin bundling and prolonged formation of filopodia (Terry-Lorenzo *et al.*, 2005). Together these results suggest that Nb1 is required to directly control the organization of the F-actin cytoskeleton, although we cannot rule out other indirect effects on cellular processes such as receptor trafficking. Our demonstration that in vivo loss of Nb1 alters the shape of neurons before, during, or after migration through the cortical plate, further confirms its role as a regulator of neuronal morphology.

The shRNA constructs used in our studies were designed to only target endogenous Nb1 transcripts. This strategy allowed us to attempt rescue experiments by coexpressing exogenous Nb1. Unexpectedly, cotransfected neurons exhibited a wide range of morphological defects (data not shown), suggesting that tight regulation of Nb1 levels and activity are required for normal neuronal differentiation. In confirmation, overexpression of Nb1 also perturbed neurite outgrowth and branching. Furthermore, both loss- and gain-of-function approaches resulted in dose-dependent consequences that were observed in vitro and in vivo.

The failure to correctly specify only one axon after changes in Nb1 expression can be interpreted in at least two ways. Neurons with altered Nb1 may develop slower than controls and therefore display a delayed separation of axonal and dendritic compartments. This hypothesis is sup-

**Figure 8 (cont).** intermediate zone (IZ), in deep layers (V–VI) and in superficial layers (II–IV) revealed that Nb1A95 is affecting neuronal migration in a less dramatic manner than wild-type Nb1 ($^{*}p < 0.001$, $^{\#}p < 0.01$, $^{\S}p < 0.05$, ns: nonsignificant). Size bars, (A–C) 25 $\mu$m; (E) 100 $\mu$m.

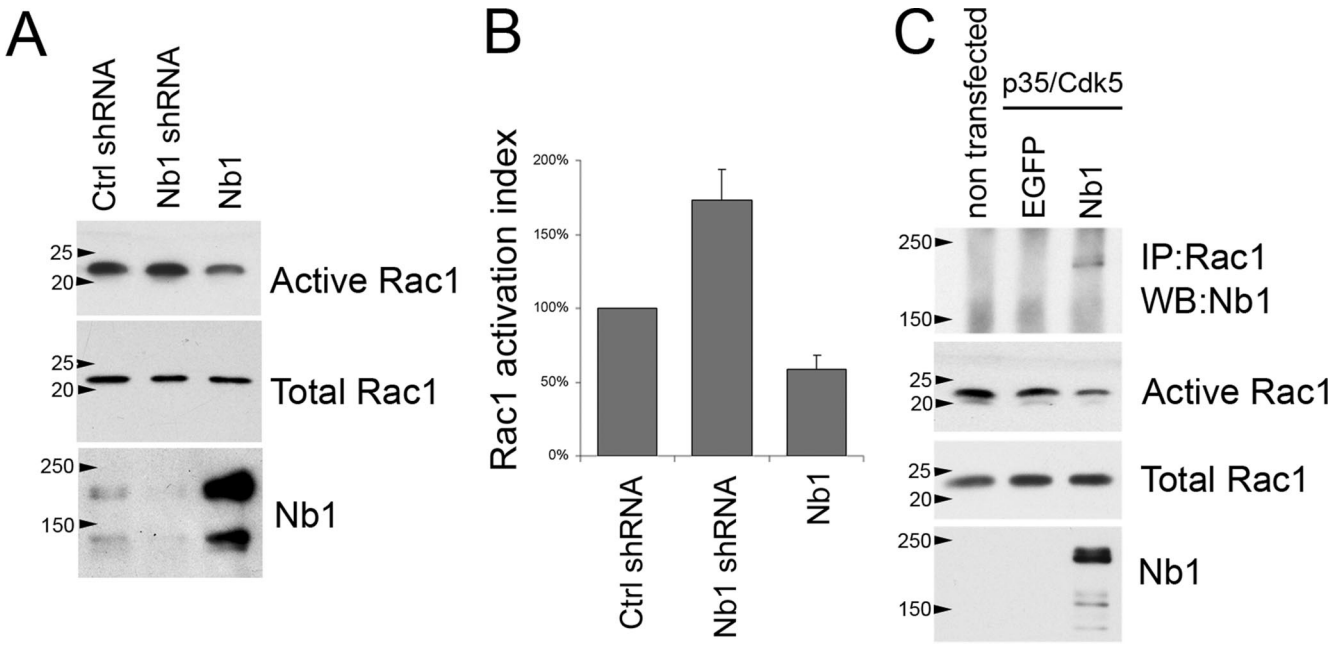


**Figure 9.** Nb1 expression levels regulate Rac1 activation. (A) Cortical neurons were transfected with control shRNA, Nb1 shRNA, or Nb1 expression constructs and lysed after 3 d in culture. The amount of Nb1, active (GTP-bound) Rac1, and total Rac1 were assessed by Western blot. (B) Quantifications of the levels of Rac1 activation revealed that down-regulation of Nb1 increased Rac1 activation, whereas Nb1 overexpression decreased it. (C) Lysates from nontransfected Cos7 cells or cells transfected with p35, Cdk5, and GFP or Nb1 expression constructs were subjected to immunoprecipitation with an anti-Rac1 antibody followed by Western blotting with an anti-Nb1 antibody. Nb1 specifically coimmunoprecipitated with endogenous Rac1. The same extracts were also used to show that Nb1 overexpression in Cos7 cells decreases activation of endogenous Rac1.

ported by our findings that loss or gain of Nb1 function reduced outgrowth of all neurites to a similar degree, suggesting that Nb1 does not preferentially regulate rapid axonal outgrowth. Furthermore, in vivo neurons overexpressing Nb1 were able to orient correctly and migrate into the cortical plate, suggesting a migration delay rather than complete arrest. Alternatively, Nb1 may act directly on the signaling cascades responsible for axonal specification. This hypothesis is strengthened by a recent study from Hung *et al.* (2007). The authors identified the *C. elegans* Nb1 homologue, NAB-1, as a key player in the restriction of axonal fate to only one neurite. This function of NAB-1 requires interaction with the SAD-1 kinase, the mouse homologues of which (SAD-A and -B) are essential for the establishment of polarity in forebrain neurons (Kishi *et al.*, 2005). Further studies will be required to address the molecular involvement of Nb1 during axonal/dendritic specification in mammals.

In the developing cerebral cortex, the highest levels of Nb1 coincide with stages of maximal neuronal migration and neurite outgrowth, suggesting its involvement in these processes. Interestingly, loss of Nb1 expression had a more severe consequence on neuronal migration than gain-of-function. Thus at P0 when most of the GFP-expressing controls resided in the peripheral region of the cerebral cortex, overexpression of Nb1 increased the number of neurons located in deeper layers of the CP and upper region of the IZ. In contrast, loss of Nb1 caused neurons to predominantly arrest in the IZ, indicative of their inability to enter the CP. These results suggest that the morphological defects induced by reduced or absent Nb1 expression are more severe than those caused by gain-of-function. Alternatively, Nb1 may have an essential role during neuronal migration that is not affected by increases in Nb1 expression and is separate from its effects on neuronal morphology. In confirmation, neurons that had stalled in the IZ appeared more fluorescent than ones that had successfully migrated to layers II–IV, indicating a correlation between shRNA expression levels and the degree of neuronal migration. We conclude that low levels of Nb1 are sufficient to enable neuronal migration, whereas full expression is required for correct morphology.

A recent report suggested that deletion of the *nb1* gene in mice does not result in any gross brain abnormalities; however the study did not include a detailed analysis of neuronal migration in the neocortex (Allen *et al.*, 2006). Importantly, mice can tolerate severe defects in cortical structure with no immediate and striking phenotype, as illustrated by the *p35* knockout model where the laminar organization of the cortex is largely inverted but the mice are viable, fertile, and only exhibit sporadic seizures (Chae *et al.*, 1997). Furthermore, acute and chronic loss of gene expression need not result in the same phenotypes. For instance, mice lacking the doublecortin gene *dcx* do not exhibit defects in cortical formation (Corbo *et al.*, 2002), whereas loss of *dcx* after shRNA expression demonstrated the essential role of doublecortin for radial migration of cortical pyramidal neurons (Bai *et al.*, 2003). A similar explanation may account for the differences between neurons in *nb1* knockout mice and those targeted with shRNAs.

Rac1 is an essential regulator of neuronal morphology, polarity, migration, pathfinding and synaptic function (Luo, 2000; Lundquist, 2003; Negishi and Katoh, 2005; Pinheiro and Gertler, 2006). Our demonstration that changes in the levels of Nb1 affect Rac1 activation, are therefore very important. The fact that increased expression of Nb1 causes a reduction of Rac1-GTP, whereas decreased Nb1 has the opposite consequence suggests that Nb1 can act as a negative regulator of Rac1. This finding is particularly interesting

considering that Nb1 associates with two Rac1 GEFs, Lfc and Kalirin (Penzes *et al.*, 2001; Ryan *et al.*, 2005). It may be that in differentiating neurons Nb1 regulates the levels of active Rac1 at the F-actin cytoskeleton, thus enabling controlled neurite outgrowth by selective activation of specific downstream signaling pathways. Changes in Nb1 levels act to disrupt this balance leading to reduced and disrupted outgrowth. The demonstration that Nb1 modulates the neurite promoting function of Rac3, whereas Neurabin II/Spinophilin can influence effector specification by Rac1, further support this hypothesis (Orioli *et al.*, 2006; Buchsbaum *et al.*, 2003).

Another important finding is the demonstrated regulation of Nb1 by the Cdk5 kinase, an essential regulator of the developing nervous system the loss of which causes embryonic lethality and a number of morphological, migratory, and functional defects in differentiating neurons (Xie *et al.*, 2006). Interestingly, Neurabin-II/Spinophilin is phosphorylated on residues S94 and S177 by PKA (Hsieh-Wilson *et al.*, 2003), S15 and S205 are modified by ERK2 (Futter *et al.*, 2005), and S100 and S116 are targeted by CaMKII (Grossman *et al.*, 2004). In all cases, phosphorylation regulates binding to F-actin. Our data now reveal that Cdk5 affects the function of Nb1 in a similar manner. Cdk5 was recently shown to phosphorylate Neurabin-II/Spinophilin on S17; however no defects were observed in the binding of Neurabin-II/Spinophilin to F-actin (Futter *et al.*, 2005). Our results imply that unlike Neurabin-II/Spinophilin, Nb1 is not targeted by Cdk5 on S17, although we only examined this reaction in vitro, and thus cannot completely rule out the possibility of it occurring in vivo.

Mutation of Nb1 on S95 to a nonphosphorylatable alanine reduced the severity of Nb1 overexpression on neuronal morphology and migration. These results indicate that 1) part of the effects of Nb1 overexpression are due to S95 phosphorylation and 2) S95-phosphorylated Nb1 affects differentiating neurons more than dephosphorylated Nb1. Nb1 associates with several key signaling proteins, which it localizes to the F-actin cytoskeleton. Consequently, by regulating the ability of Nb1 to associate with F-actin, Cdk5 may influence the activity and localization of complex signaling networks. Interestingly, in neurons Cdk5 is found complexed with Rac1 (Nikolic *et al.*, 1998) and can affect Rac1 activation by RasGRF2 and Trio (Kesavapany *et al.*, 2004; Xin *et al.*, 2004). The fact that Nb1 influences the levels of Rac1-GTP, whereas Cdk5 can modify the function of Nb1, suggests that a tightly balanced relationship between these molecules accounts for the cytoskeletal changes required for neurite outgrowth and neuronal migration. Our future work is designed to address these important points.

## ACKNOWLEDGMENTS

The authors thank Yoshimi Takai (Osaka University) for the Nb1-expressing vectors, David Turner (University of Michigan) for the shRNA expression vector, Junichi Miyazaki and Takeshi Kawauchi (Kyoto University) for pCAG-IRES-EGFP, Steve Bolsover (University College London), Deanna Taylor and Grisha Pirianov (Imperial College London) for help with actin polymerization assays, and Sonja Rakic and John Parnavelas (University College London) for invaluable technical help and support. This work was supported by the Wellcome Trust. F.C. is recipient of a European Molecular Biology Organization long-term fellowship.

## REFERENCES

Allen, P. B. *et al.* (2006). Distinct roles for spinophilin and neurabin in dopamine-mediated plasticity. Neuroscience *140*, 897–911.

Bai, J., Ramos, R. L., Ackman, J. B., Thomas, A. M., Lee, R. V., and LoTurco, J. J. (2003). RNAi reveals doublecortin is required for radial migration in rat neocortex. Nat. Neurosci. *6*, 1277–1283.

Buchsbaum, R. J., Connolly, B. A., and Feig, L. A. (2003). Regulation of p70 S6 kinase by complex formation between the Rac guanine nucleotide exchange factor (Rac-GEF) Tiam1 and the scaffold spinophilin. J. Biol. Chem. *278*, 18833–18841.

Chae, T., Kwon, Y. T., Bronson, R., Dikkes, P., Li, E., and Tsai, L. H. (1997). Mice lacking p35, a neuronal specific activator of Cdk5, display cortical lamination defects, seizures, and adult lethality. Neuron *18*, 29–42.

Cheung, Z. H., Fu, A. K., and Ip, N. Y. (2006). Synaptic roles of Cdk5: implications in higher cognitive functions and neurodegenerative diseases. Neuron *50*, 13–18.

Corbo, J. C., Deuel, T. A., Long, J. M., LaPorte, P., Tsai, E., Wynshaw-Boris, A., and Walsh, C. A. (2002). Doublecortin is required in mice for lamination of the hippocampus but not the neocortex. J. Neurosci. *22*, 7548–7557.

Dhavan, R., and Tsai, L. H. (2001). A decade of CDK5. Nat. Rev. Mol. Cell Biol. *2*, 749–759.

Fu, W. Y. *et al.* (2007). Cdk5 regulates EphA4-mediated dendritic spine retraction through an ephexin1-dependent mechanism. Nat. Neurosci. *10*, 67–76.

Futter, M., Uematsu, K., Bullock, S. A., Kim, Y., Hemmings, H. C., Jr., Nishi, A., Greengard, P., and Nairn, A. C. (2005). Phosphorylation of spinophilin by ERK and cyclin-dependent PK 5 (Cdk5). Proc. Natl. Acad. Sci. USA *102*, 3489–3494.

Grossman, S. D., Futter, M., Snyder, G. L., Allen, P. B., Nairn, A. C., Greengard, P., and Hsieh-Wilson, L. C. (2004). Spinophilin is phosphorylated by $Ca^{2+}$/calmodulin-dependent protein kinase II resulting in regulation of its binding to F-actin. J. Neurochem. *90*, 317–324.

Hsieh-Wilson, L. C., Benfenati, F., Snyder, G. L., Allen, P. B., Nairn, A. C., and Greengard, P. (2003). Phosphorylation of spinophilin modulates its interaction with actin filaments. J. Biol. Chem. *278*, 1186–1194.

Humbert, S., Dhavan, R., and Tsai, L. (2000). p39 activates cdk5 in neurons, and is associated with the actin cytoskeleton. J. Cell Sci. *113*, 975–983.

Hung, W., Hwang, C., Po, M. D., and Zhen, M. (2007). Neuronal polarity is regulated by a direct interaction between a scaffolding protein, Neurabin, and a presynaptic SAD-1 kinase in *Caenorhabditis elegans*. Development *134*, 237–249.

Kawauchi, T., Chihama, K., Nabeshima, Y., and Hoshino, M. (2003). The in vivo roles of STEF/Tiam1, Rac1 and JNK in cortical neuronal migration. EMBO J. *22*, 4190–4201.

Kawauchi, T., Chihama, K., Nabeshima, Y., and Hoshino, M. (2006). Cdk5 phosphorylates and stabilizes p27kip1 contributing to actin organization and cortical neuronal migration. Nat. Cell Biol. *8*, 17–26.

Kesavapany, S. *et al.* (2004). p35/cyclin-dependent kinase 5 phosphorylation of ras guanine nucleotide releasing factor 2 (RasGRF2) mediates Rac-dependent extracellular signal-regulated kinase 1/2 activity, altering RasGRF2 and microtubule-associated protein 1b distribution in neurons. J. Neurosci. *24*, 4421–4431.

Kim, Y. *et al.* (2006). Phosphorylation of WAVE1 regulates actin polymerization and dendritic spine morphology. Nature *442*, 814–817.

Kishi, M., Pan, Y. A., Crump, J. G., and Sanes, J. R. (2005). Mammalian SAD kinases are required for neuronal polarization. Science *307*, 929–932.

Lew, J., Beaudette, K., Litwin, C. M., and Wang, J. H. (1992). Purification and characterization of a novel proline-directed protein kinase from bovine brain. J. Biol. Chem. *267*, 13383–13390.

Lundquist, E. A. (2003). Rac proteins and the control of axon development. Curr. Opin. Neurobiol. *13*, 384–390.

Luo, L. (2000). Rho GTPases in neuronal morphogenesis. Nat. Rev. Neurosci. *1*, 173–180.

McAvoy, T., Allen, P. B., Obaishi, H., Nakanishi, H., Takai, Y., Greengard, P., Nairn, A. C., and Hemmings, H. C., Jr. (1999). Regulation of neurabin I interaction with protein phosphatase 1 by phosphorylation. Biochemistry *38*, 12943–12949.

Meyerson, M., Enders, G. H., Wu, C. L., Su, L. K., Gorka, C., Nelson, C., Harlow, E., and Tsai, L. H. (1992). A family of human cdc2-related protein kinases. EMBO J. *11*, 2909–2917.

Myat, A., Henrique, D., Ish-Horowicz, D., and Lewis, J. (1996). A chick homologue of Serrate and its relationship with Notch and Delta homologues during central neurogenesis. Dev. Biol. *174*, 233–247.

Nakanishi, H., Obaishi, H., Satoh, A., Wada, M., Mandai, K., Satoh, K., Nishioka, H., Matsuura, Y., Mizoguchi, A., and Takai, Y. (1997). Neurabin: a novel neural tissue-specific actin filament-binding protein involved in neurite formation. J. Cell Biol. *139*, 951–961.

Negishi, M., and Katoh, H. (2005). Rho family GTPases and dendrite plasticity. Neuroscientist *11*, 187–191.

Nikolic, M., Chou, M. M., Lu, W., Mayer, B. J., and Tsai, L. H. (1998). The p35/Cdk5 kinase is a neuron-specific Rac effector that inhibits Pak1 activity. Nature *395*, 194–198.

Obenauer, J. C., Cantley, L. C., and Yaffe, M. B. (2003). Scansite 2.0: proteome-wide prediction of cell signaling interactions using short sequence motifs. Nucleic Acids Res. *31*, 3635–3641.

Ohshima, T., Ward, J. M., Huh, C. G., Longenecker, G., Veeranna, Pant, H. C., Brady, R. O., Martin, L. J., and Kulkarni, A. B. (1996). Targeted disruption of the cyclin-dependent kinase 5 gene results in abnormal corticogenesis, neuronal pathology and perinatal death. Proc. Natl. Acad. Sci. USA *93*, 11173–11178.

Oliver, C. J., Terry-Lorenzo, R. T., Elliott, E., Bloomer, W. A., Li, S., Brautigan, D. L., Colbran, R. J., and Shenolikar, S. (2002). Targeting protein phosphatase 1 (PP1) to the actin cytoskeleton: the neurabin I/PP1 complex regulates cell morphology. Mol. Cell. Biol. *22*, 4690–4701.

Orioli, D., Colaluca, I. N., Stefanini, M., Riva, S., Dotti, C. G., and Peverali, F. A. (2006). Rac3-induced neuritogenesis requires binding to Neurabin I. Mol. Biol. Cell *17*, 2391–2400.

Penzes, P., Johnson, R. C., Sattler, R., Zhang, X., Huganir, R. L., Kambampati, V., Mains, R. E., and Eipper, B. A. (2001). The neuronal Rho-GEF Kalirin-7 interacts with PDZ domain-containing proteins and regulates dendritic morphogenesis. Neuron *29*, 229–242.

Pinheiro, E. M., and Gertler, F. B. (2006). Nervous Rac: DOCK7 regulation of axon formation. Neuron *51*, 674–676.

Rakic, S., Davis, C., Molnar, Z., Nikolic, M., and Parnavelas, J. G. (2006). Role of p35/Cdk5 in preplate splitting in the developing cerebral cortex. Cereb. Cortex *16*, i35–i45.

Rashid, T., Banerjee, M., and Nikolic, M. (2001). Phosphorylation of Pak1 by the p35/Cdk5 kinase affects neuronal morphology. J. Biol. Chem. *276*, 49043–49052.

Ryan, X. P., Alldritt, J., Svenningsson, P., Allen, P. B., Wu, G. Y., Nairn, A. C., and Greengard, P. (2005). The Rho-specific GEF Lfc interacts with neurabin and spinophilin to regulate dendritic spine morphology. Neuron *47*, 85–100.

Songyang, Z. *et al.* (1996). A structural basis for substrate specificities of protein Ser/Thr kinases: primary sequence preference of casein kinases I and II, NIMA, phosphorylase kinase, calmodulin-dependent kinase II, CDK5, and Erk1. Mol. Cell. Biol. *16*, 6486–6493.

Stephens, D. J., and Banting, G. (2000). In vivo dynamics of the F-actin-binding protein neurabin-II. Biochem. J. *345*, 185–194.

Tanaka, T., Serneo, F. F., Tseng, H. C., Kulkarni, A. B., Tsai, L. H., and Gleeson, J. G. (2004). Cdk5 phosphorylation of doublecortin ser297 regulates its effect on neuronal migration. Neuron *41*, 215–227.

Terry-Lorenzo, R. T., Roadcap, D. W., Otsuka, T., Blanpied, T. A., Zamorano, P. L., Garner, C. C., Shenolikar, S., and Ehlers, M. D. (2005). Neurabin/protein phosphatase-1 complex regulates dendritic spine morphogenesis and maturation. Mol. Biol. Cell *16*, 2349–2362.

Xie, Z., Sanada, K., Samuels, B. A., Shih, H., and Tsai, L. H. (2003). Serine 732 phosphorylation of FAK by Cdk5 is important for microtubule organization, nuclear movement, and neuronal migration. Cell *114*, 469–482.

Xie, Z., Samuels, B. A., and Tsai, L. H. (2006). Cyclin-dependent kinase 5 permits efficient cytoskeletal remodeling—a hypothesis on neuronal migration. Cereb. Cortex *16* (Suppl. 1), i64–68.

Xin, X., Ferraro, F., Back, N., Eipper, B. A., and Mains, R. E. (2004). Cdk5 and Trio modulate endocrine cell exocytosis. J. Cell Sci. *117*, 4739–4748.

Yu, J. Y., DeRuiter, S. L., and Turner, D. L. (2002). RNA interference by expression of short-interfering RNAs and hairpin RNAs in mammalian cells. Proc. Natl. Acad. Sci. USA *99*, 6047–6052.

Zito, K., Knott, G., Shepherd, G. M., Shenolikar, S., and Svoboda, K. (2004). Induction of spine growth and synapse formation by regulation of the spine actin cytoskeleton. Neuron *44*, 321–334.